Synthesis and characterization of sputtered nanostructured ZnO films: Effect of deposition time and pressure on contact angle behavior of ethylene glycol and water

Kartik H. Patel[1], **Sushant K. Rawal**[2*]

[1]*CHAMOS Matrusanstha, Department of Mechanical Engineering, Chandubhai S. Patel Institute of Technology (CSPIT), Charotar University of Science and Technology (CHARUSAT), Changa, 388421, India*
[2]*McMaster Manufacturing Research Institute, Department of Mechanical Engineering, McMaster University, 1280 Main Street West, Hamilton, ON, L8S 4L7, Canada*

[*]Corresponding author, Tel: (+1) 647 673 8701; E-mail: sushantrawal@outlook.com

Received: 09 February 2016, Revised: 04 August 2016 and Accepted: 22 November 2016

DOI: 10.5185/amlett.2017.6472
www.vbripress.com/aml

Abstract

This paper is aimed to explore structural, optical and wettability aspects of zinc oxide (ZnO) nanostructured thin films prepared by radio frequency (RF) magnetron sputtering from a zinc target using gas mixtures of helium and oxygen. The increase of deposition time from 40 to 110 minutes improves evolution of (100), (002) and (110) peaks for ZnO films whereas its (101) peak is evident at deposition time of 110 minutes. At sputtering pressure of 0.5Pa only (100) and (110) peaks are observed. The crystallinity of ZnO films decreases as the sputtering pressure is increased from 0.5 to 8.0Pa. The average crystallite size of films increases from 14nm to 18nm when deposition time is increased from 40 to 110 minutes and from 11nm to 17nm when deposition pressure is raised from 0.5Pa to 8.0Pa. We have studied wettability of water and ethylene glycol for deposited nanostructured ZnO films. The maximum value of contact angle; transmission and energy band gap were 106˚, 87% and 3.27eV respectively for deposited nanostructured thin films. Copyright © 2016 VBRI Press.

Keywords: ZnO, sputtering, optical, wettability, contact angle.

Introduction

ZnO has a unique position among transparent conductive oxides (TCO) due to its superior and diverse electrical, chemical, optical and magnetic properties [**1-5**]. ZnO is a transparent semiconductor with a wide band gap (3.3eV) and a large exciton binding energy of 60meV. ZnO is an eminent candidate for semiconductor materials, piezoelectric devices, photoconductors and optical waveguides [**6**]. ZnO thin films play an important role in various technological areas, such as transparent conducting thin films/electrodes in display devices and solar cells, piezoelectric devices, vapor gas sensor devices, surface and bulk acoustic wave devices, acoustic optical devices, light-emitting diodes and laser diodes due to their good bond strength, optical quality, extreme stability of excitons and excellent piezoelectric properties [**7-8**]. ZnO has many potential application like thin film transistors (TFTs), ultraviolet resistive coatings, gas sensors and mobile phones.

Wettability has substantiated to be an important property of solid surfaces and has subsequently growing research interest in the last few years. Wetting properties can be modified by deploying the morphology and chemistry of any substrate. The control of wettability is very useful for many applications as it would be constructive to be able to modify between hydrophilicity and hydrophobicity [**9, 10**].

In this work, ZnO nanostructured thin films have been deposited by RF magnetron sputtering on corning glass substrates at 300°C by using metallic target of zinc; as ZnO target is approximately 2.5 times costly than of metallic zinc target. The objective of this research work is to deposit ZnO films at different deposition time and sputtering pressure using helium and oxygen mixture. The structural, optical and wettability properties of ZnO films is examined that varies as a function of these variables. We have developed transparent ZnO films that exhibit hydrophobic behavior for water and whose affinity for ethylene glycol decreases as the deposition time and sputtering pressure is increased. The objective of the current work is to develop transparent hydrophobic ZnO nanostructured thin films by reactive RF magnetron sputtering. The novelty of this work is aimed to explore specifically the effect of helium gas, deposition time and sputtering pressure on structural, optical and wettability properties of ZnO nanostructured thin films.

Experimental

Custom designed 16” diameter × 14” cylindrical chamber (Excel Instruments, India) was used for preparing ZnO nanostructured thin films by RF magnetron sputtering. Zinc (Zn) target (Givana Tech LLC, USA) of 2” diameter with purity of 99.99%, was kept at a distance of 50mm from substrate. Helium (purity 99.999%) was used as inert gas, the flow of helium was kept constant at 12.5 sccm which was controlled using mass flow controller (Alicat, USA). Oxygen was used as reactive gas which was kept constant at 7.5 sccm. The deposition was carried out at constant RF power of 150W and deposition temperature of 300°C. ZnO nanostructured thin films were deposited at different deposition time of 40, 50, 70, 90 and 110 minutes at deposition pressure of 2.0Pa; their sample names are 40T, 50T, 70T, 90T and 110T respectively. The second set was deposited at pressure of 0.5, 3.5, 5.0, 6.5 and 8.0Pa at constant deposition time period of 60 minutes their sample names are 0.5P, 3.5P, 5.0P, 6.5P and 8.0P respectively. The reaction occurred inside the chamber is given as follow:

$$\mathrm{Zn}^{2+} + \mathrm{O}^{2-} \rightarrow \mathrm{ZnO}$$

The structural properties of ZnO nanostructured thin films were studied by X-ray diffractometer (XRD) (Bruker, Model D2 Phaser). The wettability properties of ZnO thin films were examined by contact angle measuring system with accuracy of ± 2° (Ramehart, Model 290). Atomic force microscopy (Nanosurf easy scan 2) was utilized to characterize its surface topography. The optical properties like transmission and energy band gap of ZnO nanostructured thin films were recorded by UV-vis-NIR spectrophotometer (Shimadzu, Model UV-3600 plus).

Results and discussion

The XRD graphs of ZnO nanostructured thin films synthesized at various deposition times of 40, 50, 70, 90 and 110 minutes are shown in **Fig. 1(a)**. **Fig 1(b)** shows the XRD graphs of ZnO thin films at different sputtering pressure of 0.5, 3.5, 5.0, 6.5 and 8.0 Pa. At deposition time of 40 minutes, (100) and (002) peaks of ZnO along with its weakly crystalline (110) peak is observed. The evolution of (101) peak is observed from deposition time of 50 minutes; the intensity of (101) peak along with (110) peak increases as deposition time is increased to 110 minutes. When the deposition time is increased from 40 to 110 minutes, the intensity of (100) and (002) peaks of ZnO is also enhanced. This indicates that increasing deposition time enhances crystallization of ZnO thereby resulting in formation of ZnO nanostructured thin films having different orientations.

In other set of experiment when sputtering pressure was varied, only (100) and (110) peaks of ZnO is observed at sputtering pressure of 0.5Pa indicating formation of weakly crystalline ZnO nanostructured thin films. The evolution of (002) texture is observed from sputtering pressure of 3.5 Pa, its maximum intensity is observed at 5.0Pa thereby a decline in its intensity is observed from 6.5 to 8.0 Pa. When the sputtering pressure has higher values of 6.5 Pa and 8.0 Pa the intensity of various ZnO textures diminishes gradually. P.F. Yang *et al.* [**11**] prepared ZnO thin films in argon and oxygen mixtures at 200W, 0.8 mPa, and 200 °C for different deposition time of 60, 120 and 180 minutes. They observed only (002) peak of ZnO at 60 minutes, its (100) and (002) peaks at 120 minutes and (100), (002) and weakly crystalline (101) peak of ZnO at 180 minutes.

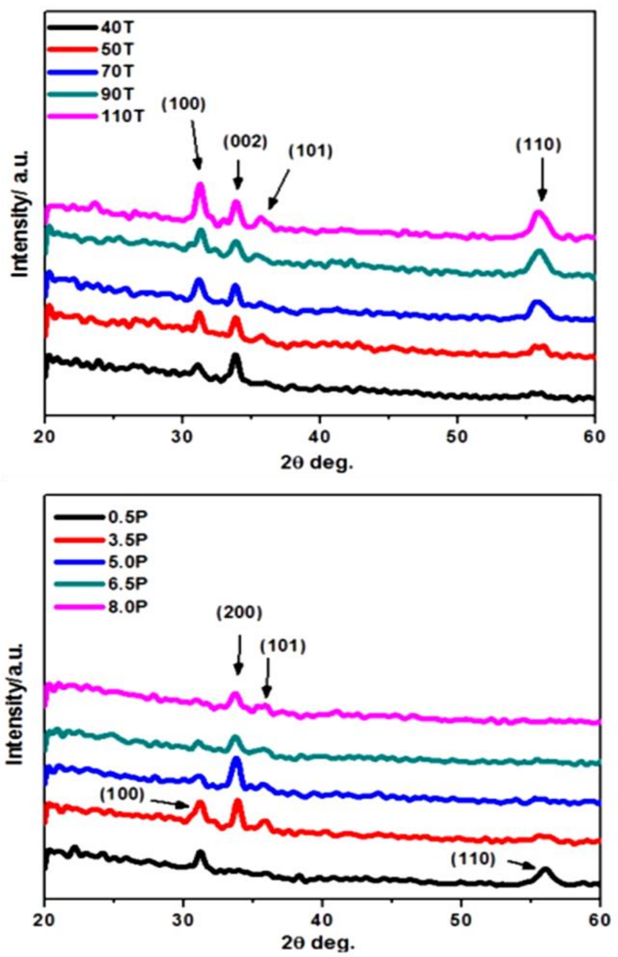

Fig. 1. XRD patterns of the ZnO films at different (a) Deposition Time and (b) Sputtering Pressure.

N. Tang *et al.* [**12**] deposited ZnO thin films at constant power of 200W using argon and oxygen gas and at different working pressure of 1.0, 1.5, 2.0 and 3.0 Pa. They observed only (002) peak of ZnO and detected that its intensity increases when pressure is increased from 1.0 to 2.0 Pa. The further increase of pressure to 3.0 Pa leads to decline in intensity of (002) peak forming weakly crystalline ZnO films.

Table1. Calculated parameters of nanostructured zinc oxide thin films.

Sample name	RF power (W)	Temperature (˚C)	Avg $d_{(XRD)}$ (nm)	Band gap (eV)	Refractive index (n)	Thickness (nm) by %T data
40T	150	300	14	3.27	1.509	479
50T	150	300	15	3.26	1.505	723
70T	150	300	16	3.24	1.505	920
90T	150	300	17	3.23	1.505	937
110T	150	300	18	3.21	1.503	1357
0.5P	150	300	11	3.21	1.507	899
3.5P	150	300	14	3.22	1.507	885
5.0P	150	300	14	3.24	1.508	836
6.5P	150	300	16	3.25	1.509	708
8.0P	150	300	17	3.27	1.509	502

In our first set of experiment, when deposition time is varied from 40 to 110 minutes we could obtain well crystalline ZnO films having (100), (002), (101) and (110) textures at lower power value of 150 W. In our second set of experiment, when the sputtering pressure was varied from 0.5 to 8.0 Pa we could successfully obtain (100), (002), (101) and (110) textures of ZnO at 3.5 Pa sputtering pressure. Even at higher sputtering pressure range from 5.0 to 8.0 Pa we could achieve (002) and (101) peak of ZnO. This indicates that when working pressure is around 3.0Pa, it favors crystallization of ZnO, thereby resulting in formation of ZnO thin films having different orientations. The major reason for formation of crystalline ZnO films may be due to usage of helium as an inert gas during deposition. As reported in literatures [**13-15**], helium has higher ionization energy as compared to argon that favors formation of metal oxide films even at lower flow rate of oxygen. The average crystallite size of ZnO films as calculated by Scherrer formula [**16**] is given in **Table 1**. The average crystallite size increases from 14nm to 18 nm when deposition time is increased from 40 to 110 minutes and from 11 to 17nm when deposition pressure is raised from 0.5 Pa to 8.0 Pa.

The loss of c-axis preference when mixture of He-O_2 gas is used may be due to penning ionization process that occurs in plasma. Helium (He) has highest energy than the first ionization potential of O_2 and therefore it can effortlessly ionize the latter. So when ZnO thin films are deposited in He-O_2 mixtures, there will be more amounts of O_2 atoms accessible that may have caused in development of various textures of ZnO thin films and resulted in lesser c-axis preference with evolution of other orientations.

Contact angle θ is defined as the angle between the liquid-vapor interface and the solid surface, measured through liquid at the point on surface where all three phases meet. The contact angle is not a fluid property but rather a function of fluid's free surface energy as compared to solid surface and vapor surface energies [**17**].

A smaller contact angle means that more of fluid spreads over an area for a given fluid volume; hence fluid has a high wettability on that surface. Fluids with $\theta = 0°$ are called highly wetting and with $\theta = 180°$ are called highly non-wetting. In case of heat pipes, maximum capillary pressure is reached when $\theta = 0°$ for a working fluid [**18**]. For surfaces that are real or surfaces that are rough and/or heterogeneous, contact angle depends on the point where it is measured.

The AFM micrographs of ZnO nanostructured thin films deposited at different deposition time and sputtering pressure are shown in **Fig**. **2**. The average crystalline size increases with increase in deposition time and pressure which is visible from AFM micrographs thereby confirming XRD results.

Ethylene glycol is good antifreeze agent and coolant for many commercial and industrial applications. In many industrial systems like air-conditioning, gas compressors, thermal solar energy and heating, it is used as heat transfer fluids. The better contact angle of ethylene glycol is advantageous in corrosion inhibitor through cleaning after metal chemical mechanical polishing [**19-21**].

The contact angle of water and ethylene glycol was measured by sessile drop method. **Fig. 3a** and **3b** shows contact angle values for water and ethylene glycol with respect to surface roughness of zinc oxide nanostructured thin films. When deposition time is varied from 40 to 110 minutes, the surface roughness of ZnO nanostructured thin films is increased from 23 to 40 nm; the contact angle of water is increased from 70° to 106° and of ethylene glycol is improved from 50.4° to 74.2°. When the sputtering pressure is increased from 0.5 to 8.0Pa, the surface roughness is raised from 24 to 36 nm which leads to higher contact angle of water from 80° to 104° whereas for ethylene glycol contact angle varies from 60° to 73.4°.

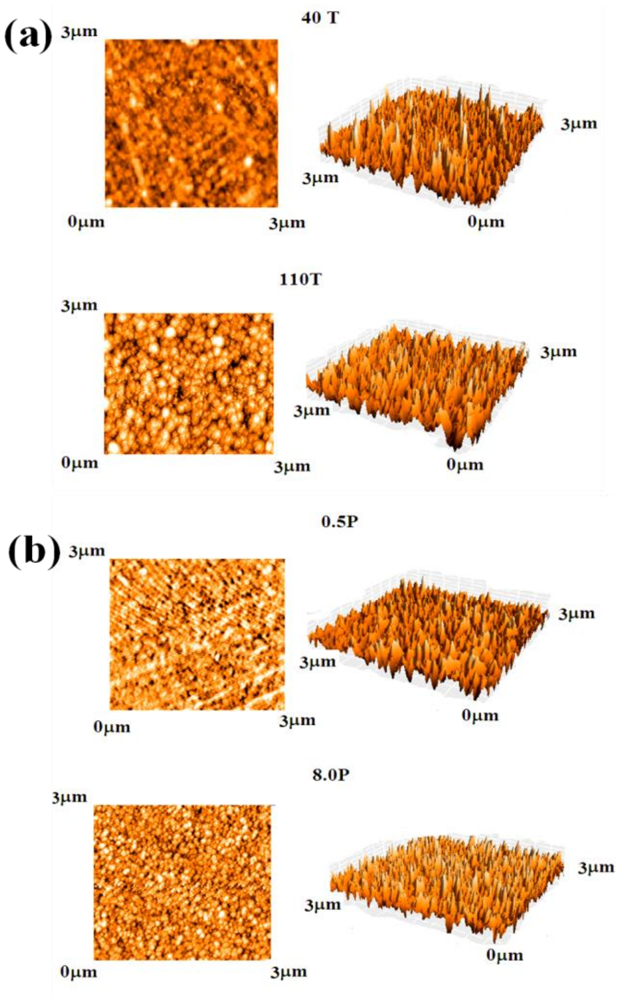

Fig. 2. AFM images of the ZnO films deposited at different (a) Deposition Time and (b) Sputtering Pressure.

The wetting behavior of a thin film is not only characterized by static contact angle but also by dynamic contact angle. Contact Angle Hysteresis (CAH) is the variance between advancing contact angle (θ_A) and receding contact angle (θ_R) that is measured while determining dynamic contact angle. The contact angle hysteresis is associated to surface roughness and adhesion of droplet to the surface [**22**]. The values of advancing contact angle (θ_A), receding contact angle (θ_R) and CAH for water and ethylene glycol are shown in **Table 2**. When deposition time of ZnO nanostructured thin films is increased from 40 to 110 minutes, CAH of water decreases from 11° to 3.1° and for ethylene glycol decline of values from 14.6° to 9.1° is observed. CAH for water declines from 10° to 6.8° and for ethylene glycol from 15° to 10.2° when sputtering pressure of ZnO nanostructured thin films is raised from 0.5Pa to 8.0Pa.

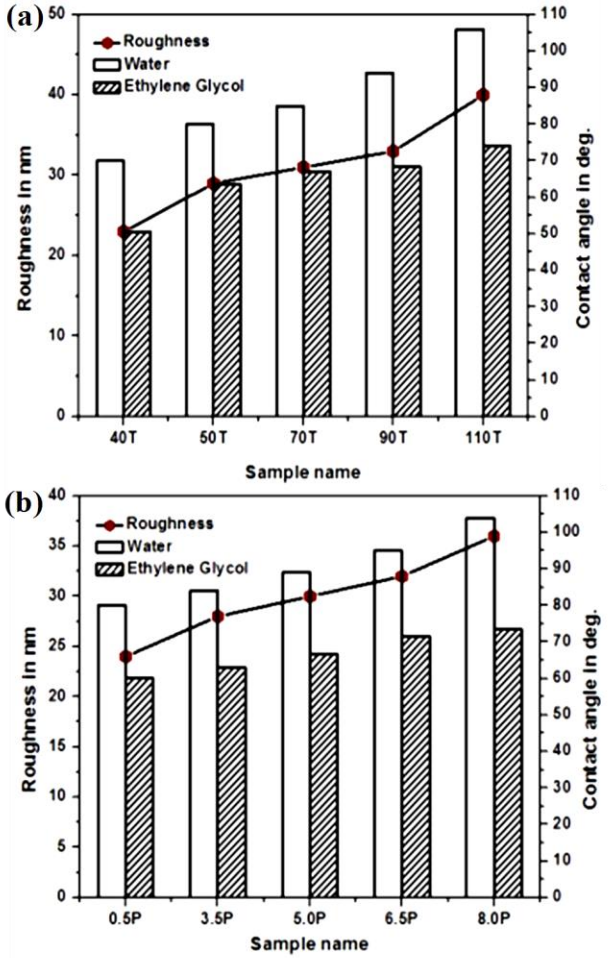

Fig. 3. Contact angle and surface roughness of ZnO films deposited at different (a) Deposition Time and (b) Sputtering Pressure.

We obtained lowest CAH values of 3.1° and 9.1° for water and ethylene glycol respectively at maximum surface roughness value of 40nm at deposition time of 110 minutes for deposited ZnO nanostructured thin films. The liquid gets easily rolled on that surface when it's slightly tilted from horizontal level.

This behavior is very useful for glasses which are used in multi storage buildings and vehicles. We found that the magnitude of CAH decreases with increasing deposition time and sputtering pressure, which may be due to surface roughness.

If the surface is rough, the actual surface area is greater than uncoated surface area, so the total liquid-solid interaction is higher on rough surface than on uncoated surface. The zinc oxide nanostructured thin films show increase in their surface roughness values with an increase in deposition time and sputtering pressure.

The deposited ZnO nanostructured thin films show an increase in contact angle for water and ethylene glycol with increase in surface roughness as contact angle is directly proportionate to surface roughness.

Table. 2. Static and dynamic contact angle and contact angle hysteresis (CAH) of nanostructured zinc oxide thin films.

		Static angle (in deg.)		Dynamic angle (in deg.)					
Sample	**Roughness in nm**	**Water**	**EG**	**Water**		**EG**		**CAH**	
				θ_A	θ_R	θ_A	θ_R	**Water**	**EG**
40T	23	70	50.4	72.4	61.4	51.2	36.6	11	14.6
50T	29	80	63.6	82.4	73	65	51.4	9.4	13.6
70T	31	85	67	87.3	78.4	67.2	54.7	8.9	12.5
90T	33	94	68.3	98.1	90.5	71.3	60.3	7.6	11
110T	40	106	74.2	107.5	104.4	77.6	68.5	3.1	9.1
0.5P	24	80	60	84.5	74.3	63.8	48.8	10.2	15
3.5P	28	84	63.3	87.2	78.7	66.6	52.9	8.5	13.7
5.0P	30	89	66.6	93.3	85.8	69.8	57.3	7.5	12.5
6.5P	32	95	71.4	97.36	91.3	74.4	63.3	6.06	11.1
8.0P	36	104	73.4	108.2	101.4	77.5	67.3	6.8	10.2

Varying the surface chemical composition and surface morphology are challenging processes for surface energy of a film. Contact angle depends on surface roughness and it is inversely proportional to surface energy [**23**]. Surface energy of ZnO nanostructured thin films calculated by Owens-Wendt (O.W.) [**24-25**] and Wu method is shown in **Fig. 4a** and **4b** respectively. The surface energy of ZnO nanostructured thin films found by both methods decreases when deposition time is increased from 40 to 110 minutes and sputtering pressure is increased from 0.5 to 8.0Pa. The total surface energy which is sum of the polar γ_s^p and dispersion γ_s^d components found by two methods are in good agreement with each other.

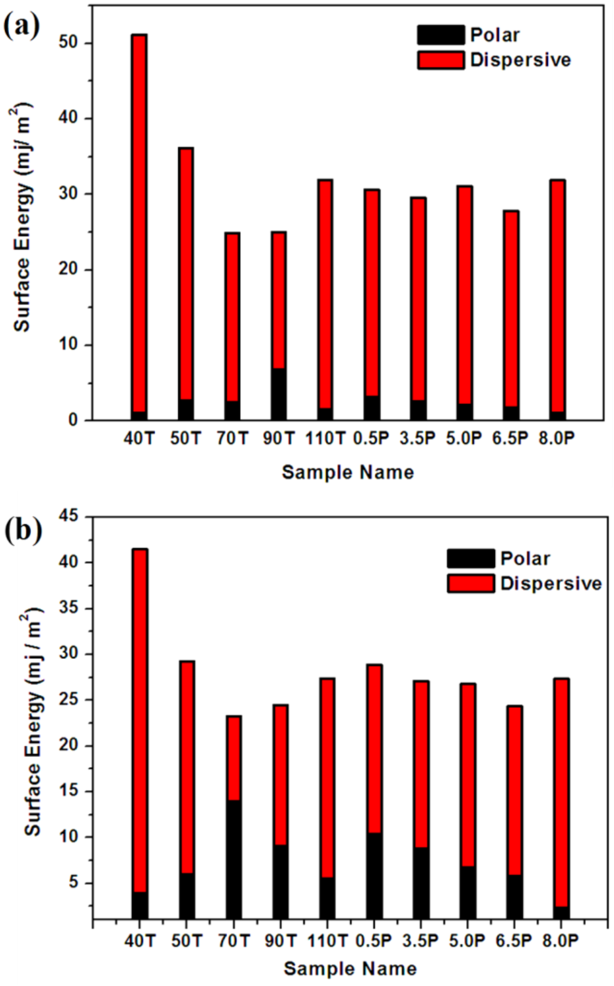

Fig. 4. Surface energies of ZnO films deposited on glass substrates calculated by (a) O.W. method and (b) Wu method.

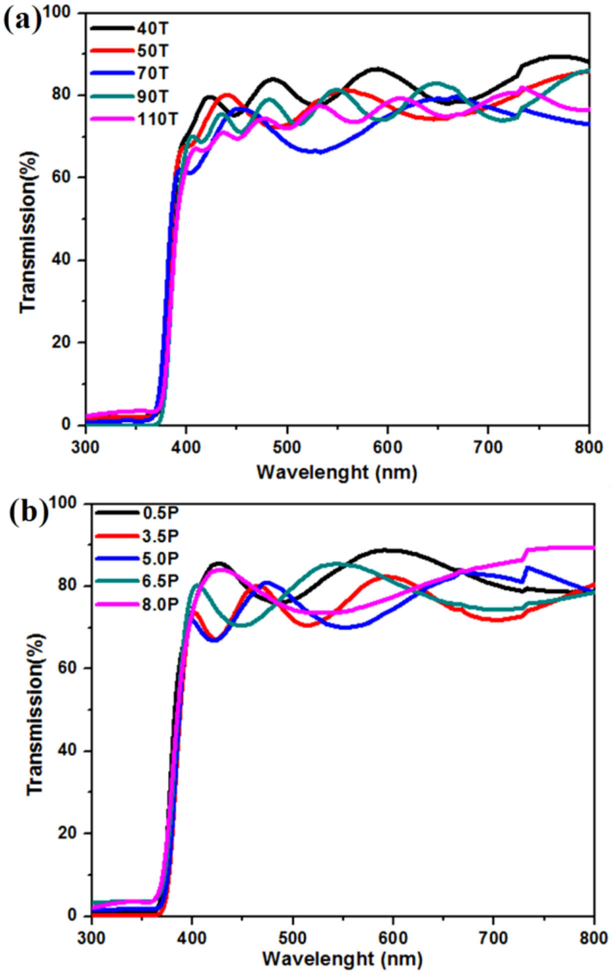

Fig. 5. Optical transmission curves of ZnO films deposited at different (a) Deposition Time and (b) Sputtering Pressure.

The highest contact angle of water and ethylene glycol for ZnO nanostructured thin films is obtained up to 106° and 74.2° for sample 110T respectively. The films deposited at these conditions are hydrophobic for water and repellency of films specifically for ethylene glycol increases from its initial value of 26º observed for uncoated substrate. So we have demonstrated the development of repellent ZnO nanostructured thin films that can be tailor made as per the requirement of specific applications involving water and ethylene glycol. It can have possible uses as hydrophobic coatings.

UV-vis-NIR spectrophotometer was used to measure transmittance and absorbance spectra for zinc oxide thin films. The transmission curves for ZnO nanostructured thin films deposited at different deposition time and sputtering pressure are shown in **Fig. 5(a)** and **5(b)** respectively. The optical transmittance ZnO nanostructured thin films was measured in the range of 300 to 800 nm. The thickness and grain size affects transmission and optical band gap values. It is clearly observed from **Fig. 5(a)** and **5(b)** that with increase in deposition time and pressure, the transmission values of ZnO films decreases. The thickness of ZnO nanostructured thin films increases with increase in deposition time and decreases with sputtering pressure. Larger crystallite size combined with high surface roughness will lead to more electrons scattering when deposition time and deposition pressure is increased. This results in decline of transmission values for ZnO thin films.

The model proposed by Manifacier *et al.* [**26**] is used to obtain refractive index of ZnO nanostructured thin films from transmission data. It is evident that the refractive index 'n' of ZnO nanostructured thin films is around 1.5 to 1.51 for variation of deposition time and deposition pressure as given in **Table 1**. To determine the optical band gap of zinc oxide films, absorption spectra of ZnO nanostructured thin films were recorded as a function of wavelength. The optical band gap (E_g) of ZnO nanostructured thin films was calculated from absorption coefficient (α) using Tauc relation [**27**].

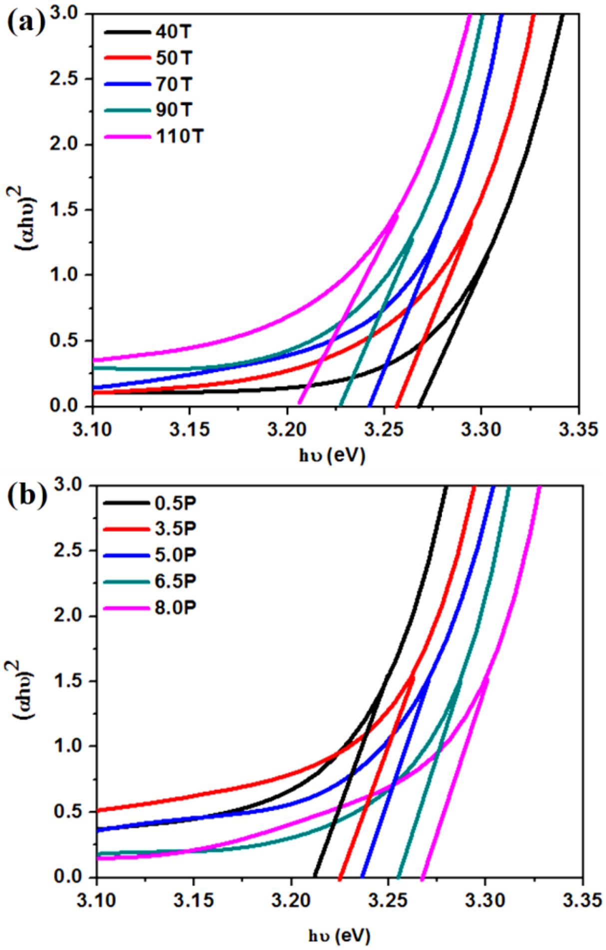

Fig. 6. Optical absorption curves of ZnO films deposited at different (a) Deposition Time and (b) Sputtering Pressure.

As reported in the literatures zinc oxide is direct band gap semiconductor [**28-29**]. **Fig. 6a** and **6b** shows plot of $(\alpha h\upsilon)^2$ on the y-axis versus photon energy $(h\upsilon)$ on x-axis for zinc oxide films. The calculated band gap values for ZnO nanostructured thin films varies from 3.27eV to 3.21eV for variation in deposition time from 40 to 110 minutes and from 3.21eV to 3.27eV for sputtering pressure variation from 0.5 to 8.0 Pa. The observed band gap values of ZnO nanostructured thin films deposited at various sputtering conditions are in good indenture with literatures [**30-31**].

Conclusion

ZnO nanostructured thin films were deposited at different values of deposition time and sputtering pressure. The deposited films exhibit (100), (002), (101) and (110) peaks of ZnO and larger grain size is observed with increase in deposition time from 40 to 110 minutes. When sputtering pressure is 3.5Pa (100), (002) and (101) textures of ZnO is observed. At deposition time of 110 minutes, ZnO nanostructured thin films have contact angle values of 106° and 74.2° for water and ethylene glycol respectively. At surface roughness of 36nm, 104° contact angle for water and 73.4° for ethylene glycol is observed at sputtering pressure is 8.0Pa. Wettability of surface depends on the surface roughness. The optical energy band gap decreases as deposition time is increased and increases as sputtering pressure of ZnO nanostructured thin films is increased.

Acknowledgements

This work has been supported by AICTE grant number 20/AICTE/RIFD/RPS (POLICY-III) 24/2012-13 sanctioned under Research Promotion Scheme (RPS). We are thankful to Head, Dr. K. C. Patel Research and Development Centre (KRADLE) affiliated to Charotar University of Science and Technology (CHARUSAT), Anand, Gujarat, India for granting permission to use various equipment's available in their characterization laboratory.

References

1. Prashanth, G.; Prashanth, P.; Bora, U.; Gadewar, M.; Nagabhushana, B.; Ananda, S.; Krishnaiah, G.; Sathyananda, H; *Karbala Inter. J. of Modern Sci.*, **2015**, *1*, 67.
   DOI: 10.1016/j.kijoms.2015.10.007
2. Ismail, A.; Abdullah, M. J.; *J. King Saud Univ., Sci.*, **2013**, *25*, 209.
   DOI: 10.1016/j.jksus.2012.12.004
3. Kamada, Y.; Mamoru, F.; Hiramatsu, T.; Kawaharamura, T.; Wang, D.; Shimakawa, S.; Li, C.; Fujita, S.; Hirao, T; *Appl. Surf. Sci.*, **2011**, *258*, 695.
   DOI: 10.1016/j.apsusc.2011.07.100
4. Sharma, D.; Ashaduzzaman, M.; Golabi, M.; Shriwastav, A.; Bisetty, K.; Tiwari, A.; *ACS Applied Materials & Interfaces*, **2015**, 7, 23848.
   DOI: 10.1021/acsami.5b06617
5. Mende, L. S.; Driscoll, J; *Mater. Today*, **2007**, *10*, 40.
   DOI :10.1016/S1369-7021(07)70078-0
6. Ghafouri, V.; Shariati, M.; Ebrahimzad, A; *Sci. Iran. F.*, **2012**, *19*, 934.
   DOI: 10.1016/j.scient.2012.04.017
7. Yuste, M.; Galindo, R. E.; Caretti, I.; Torres, R.; Sanchez, O.; *J. Phys. D. Appl. Phys.*, **2012**, *45*, 025303.
   DOI: 10.1088/0022-3727/45/2/025303
8. Toledano, D.; Galindo, R.; Yuste, M.; Albella, J.; Sanchez, O; *J. Phys. D. Appl. Phys.*, **2013**, *46*, 045306.
   DOI: 10.1088/0022-3727/46/4/045306
9. Papadopoulou, E. L.; Zorba, V.; Pagkozidis, A.; Barberoglou, M.; Stratakis, E.; Fotakis, C; *Thin Solid Films*, **2009**, *518*,1267.
   DOI: 10.1016/j.tsf.2009.02.077
10. Yildirim, E. H.; Surface chemistry of solid and liquid interfaces; Blackwell: UK, **2006**.
11. Yang, P.F.; Wen, H.C.; Jian, S. R.; Lai, Y.S.; Wu, S.; Chen, R; *Microelectron. Reliab.*, **2008**, *48*, 389.
    DOI:10.1016/j.microrel.2007.08.010
12. Ning, T.; Jinliang, W.; Hengxing, X.U.; Hongyong, P.; Chao, F; *Sci China Ser E*, **2009**, *52*, 2200.
    DOI:10.1007/s11431-009-0230-1
13. Chawla, A.K.; Singhal, S.; Gupta, H.O.; Chandra, R; *Thin Solid Films*, **2008**, *517*, 1042.
    DOI:10.1016/j.tsf.2008.06.068
14. Kruithof, A. A.; Penning, F; *Physica.*, **1937**, *4*, 430.
    DOI:10.1016/S0031-8914(37)80075-0
15. Fujii, T.; Koyanagi, T.; Morofuji, K.; Kashima, T.; Matsubara, K; *Japanese J. Appl. Phys.*, **1994**, *33*, 4482.
    DOI:10.1143/JJAP.33.4482
16. Cullity, B. D.; Elements of X-ray Diffraction; Wesley Publishing: USA, **1978**.
17. Woodruff, D. P.; The solid-liquid interface; CUP Archive, **1973**.
18. Faghri, A.; Heat pipe science and technology; Global Digital Press: Washington, DC, **1995**.
19. Xu, G. H.; Li, Y.C.; Li, Z.H.; Wang, H; *Ind. Eng. Chem. Res.*, **1995**, *34*, 2371.
    DOI: 10.1021/ie00046a020
20. Chen, L. F.; Guo, P.J.; Qiao, M. H.; Yan, S. R.; Li, H. X.; Shen, W.; Fan, K; *J. Catal.*, **2008**, *257*, 172.
    DOI:10.1016/j.jcat.2008.04.021
21. Yue, H.; Zhao, Y.; Ma, X.; Gong, J; *Chem. Soc. Rev.*, **2012**, *41*, 4218.
    DOI: 10.1039/C2CS15359A
22. Gurav, A. B.; Latthe, S. S.; Vhatkar, R.S.; Lee, J .G.; Kim, D. Y.; Park, J. J.; Yoon, S; *Ceram. Int.*, **2014**, *40*, 7151.
    DOI:10.1016/j.ceramint.2013.12.052
23. Chiu, S. M.; Hwang, S. J.; Chu, C. W.; Gan, D; *Thin Solid Films*, **2006**, *515*, 285.
    DOI:10.1016/j.tsf.2005.12.141
24. Rawal, S. K.; Chawla, A. K.; Chawla, V.; Jayaganthan, R.; Chandra, R; *Thin Solid Films*, **2011**, *519*, 7686.
    DOI:10.1016/j.tsf.2011.05.056
25. Shekhar, A.; Tiwari, A.; Shukla, S. K.; Vamakshi, Minakshi, Anand; *Advanced Materials Letters*, **2012**, 3, 421.
    DOI: 10.5185/amlett.2012.5349
26. Manifacier, J. C.; Gasiot, J.; Fillard, J; *J. Phys. E: Sci. Instrum.*, **1976**, *9*, 1002.
    DOI:10.1088/0022-3735/9/11/032
27. Tauc, J. (Ed.); Amorphous and Liquid Semiconductor; Plenium Press: NewYork, **1974.**
28. Cho, S; *Electr. Electron. Mater*., **2009**, *10*, 185.
    DOI:10.4313/TEEM.2009.10.6.185
29. Kumar, G. A.; Reddy, M. R.; Reddy, K; *Res. J. Phys. Sci.*, **2013**, *1*, 17.
30. Ondo-Ndong, R.; Moussambi, H. Z.; Gnanga, H.; Giani, A.; Foucaran, A; *Int. J. Phys. Sci.*, **2015**, *10*, 173.
    DOI:10.5897/IJPS2014.4241
31. Senay, V.; Pat, S.; Korkmaz, S.; Aydogmuş, T.; Elmas, S.; Ozen, S.; Balbag, M; *Appl. Surf. Sci.*, **2014**, *318*, 2.
    DOI:10.1016/j.apsusc.2013.10.044